Supporting Information for: Capillary assembly of microscale ellipsoidal, cuboidal, and spherical particles at interfaces

Sabyasachi Dasgupta,* Marina Katava, Mohammed Faraj, Thorsten Auth,* and Gerhard Gompper*

Theoretical Soft Matter and Biophysics, Institute of Complex Systems and Institute for Advanced Simulation, Forschungszentrum Jülich, D-52425 Jülich, Germany

E-mail: s.dasgupta@fz-juelich.de; t.auth@fz-juelich.de; g.gompper@fz-juelich.de

In this supplementary material, we present numerical data to further characterize the interface deformation around and the capillary interaction between ellipsoidal and cuboidal particles. For a contact angle $\theta_c \neq 90\,^\circ$, a constant contact angle cannot be achieved for a planar interface around an ellipsoidal particle and around a cuboidal particle with rounded edges. For $\theta_c < 90\,^\circ$, the interface is pulled down at the tips and pulled up at the sides of the ellipsoids, thereby creating excess interface area. Fig. S1 shows the deformation of the interface around an ellipsoidal particle in the directions of the long and the short axis. The deformation profiles are plotted for contact angles $\theta_c^{\max}$ that correspond to maximal interfacial distortions for the given aspect ratios of the particles. It is obvious that the interface deformation increases with increasing aspect ratio, which implies that the capillary interaction between two particles will also increase. The difference of the highest and lowest points along the contact line normalized by the minor axis of a particle, $\Delta u/a$, characterizes

*To whom correspondence should be addressed

the interface deformation in the near field. Fig. S2 shows a non-monotonic variation of $\Delta u/a$ with θ_c together with data from the literature.[1,2] Our numerical results show good agreement with the published data.

The maximal height difference $\Delta u/a$ along the undulating contact line vanishes for mirror-symmetric conditions at $\theta_c = 0°$ and $90°$, and varies non-monotonically for intermediate angles attaining a peak value $\Delta u_{\max}/a$ at particular contact angle $\theta_c^{\max}$. For ellipsoidal particles, the calculated peak value monotonically increases from $\Delta u_{\max}/a = 0.0128$ for $b/a = 1.1$ to $\Delta u_{\max}/a = 0.4307$ for $b/a = 13$. Another experimentally measurable quantity is the projected area enclosed by the undulating contact line, S, which is obtained by calculating the area enclosed by the polygon formed by the vertices of the contact line projected to the x-y plane. In Fig. S3, we plot S/S_0, where S_0 is the area enclosed by the contact line for $\theta_c = 90°$. The monotonically increasing function S/S_0 allows to single out the correct contact angle solution where Δu is ambiguous.[1]

The peak values of $\Delta u_{\max}/a$ for all aspect ratios that we have calculated and the corresponding contact angles that vary in the range $43° < \theta_c^{\max} < 55°$ are reported in Tab. S1. In Tab. S2, we report the peak values for the contact line deformation for cuboidal particles. Because of the very small variation of $\Delta u/a$ with θ_c, it is difficult to calculate the contact angles that correspond to the peak values at small aspect ratios accurately. In Tab. S3, we report the parameters obtained by fitting the numerically calculated interaction potentials in the near field to $\Delta E/\gamma a^2 = k(d_{cc}/a)^{-m}$, as well as the bond angles at contact.

Fig. S4 shows the deformation of the contact line on a spherical particle that is next to an ellipsoidal particle. The contact line at the spherical particle is pulled up if the spherical particle is located next to the side of the ellipsoid and is pulled down if the spherical particle is located next to the tip of the ellipsoid. Part of the excess area generated by the ellipsoidal particle is therefore reduced due to the presence of the spherical particle, which leads to an attractive interaction between both particles.

Table S1: Peak values $\Delta u_{\max}$ of the maximal height differences Δu along the contact line and corresponding contact angles $\theta_c^{\max}$ for ellipsoidal particles with aspect ratios in the range $1.1 \leq b/a \leq 13$.

$\mathbf{b/a}$	$\mathbf{\Delta u_{max}/a}$	$\theta_{\mathbf{c}}^{\mathbf{max}}$
1.10	0.01284	54.12°
1.25	0.0310	53.84°
1.50	0.0600	52.34°
1.75	0.0867	51.55°
2.00	0.1110	50.95°
2.25	0.1331	50.55°
2.50	0.1530	50.10°
2.75	0.1714	49.73°
3.00	0.1872	49.67°
4.00	0.2410	48.94°
5.00	0.2803	48.47°
6.00	0.3126	47.56°
7.00	0.3483	45.20°
8.00	0.3600	44.82°
9.00	0.3762	44.61°
10.00	0.3940	43.73°
11.00	0.4091	43.31°
12.00	0.4203	43.22°
13.00	0.4307	43.21°

Table S2: Peak values $\Delta u_{\max}$ of the maximal height differences Δu along the contact line and corresponding contact angles $\theta_c^{\max}$ for cuboidal particles with aspect ratios in the range $2 \leq b/a \leq 10$.

$\mathbf{b/a}$	$\mathbf{\Delta u_{max}/a}$	$\theta_{\mathbf{c}}^{\mathbf{max}}$
2.00	0.0678	62.93°
2.25	0.0806	62.73°
2.50	0.0918	61.98°
2.75	0.1030	61.63°
3.00	0.1110	61.31°
4.00	0.1417	61.11°
5.00	0.1660	60.27°
6.00	0.1850	59.38°
7.00	0.2007	58.96°
8.00	0.2147	58.36°
9.00	0.2266	56.83°
10.00	0.2375	56.47°

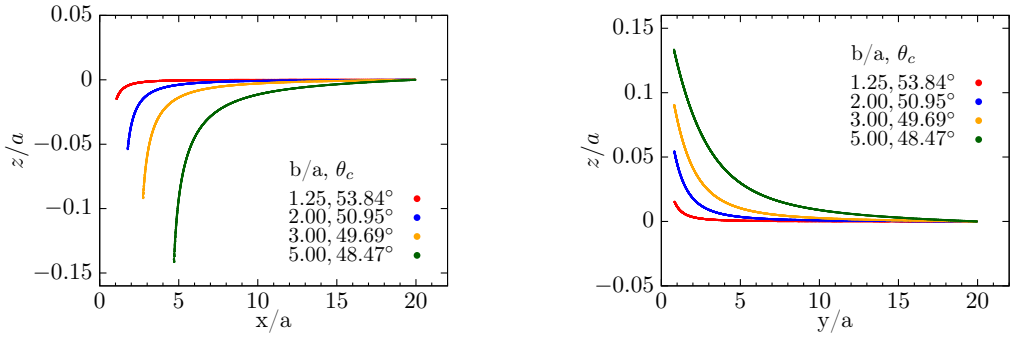

(a) (b)

Figure S1: Interface deformation around ellipsoidal particles with aspect ratios $b/a = 1.25$, $b/a = 2$, $b/a = 3$, and $b/a = 5$ in the direction of (a) their long axis along the x axis and (b) their short axis along the y axis. The contact angles have been chosen such that the difference between the highest and the lowest point of the contact line is maximal.

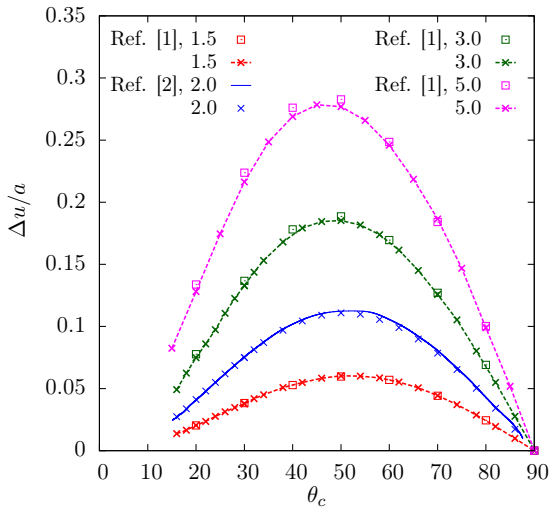

Figure S2: Maximal height difference along the contact line, Δu, as function of the contact angle θ_c for ellipsoidal particles. Our numerical data for aspect ratios $b/a = 1.5$, $b/a = 2$, $b/a = 3$, and $b/a = 5$ are plotted together with data taken from Ref. [1] and Ref. [2].

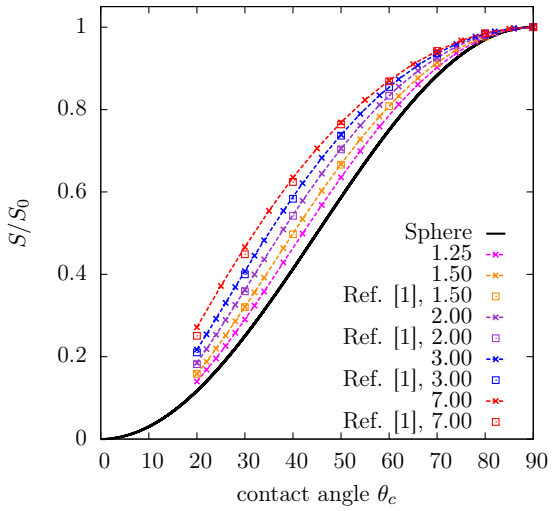

Figure S3: Ratio of projected area S enclosed by the contact line for the to the projected area enclosed by the contact line for $\theta_c = 90°$, S_0, as function of the contact angle θ_c for ellipsoidal particles with aspect ratios in the range $1.25 \leq b/a \leq 7$. Our data are plotted together with numerical data taken from Ref. [1]. For a spherical particle, S/S_0 varies as $\sin^2 \theta_c$, as shown by the solid line. For all contact angles between 0° and 90°, S/S_0 attains higher values for ellipsoidal particles in comparison to the analytical result for a spherical particle.

Table S3: Fit parameters k and m and bond energies for particles at contact obtained from the fit functions. Data for ellipsoidal and cuboidal particles in side-by-side (S-S), tip-to-tip (T-T), and tip-to-side (T-S) orientation is provided. The fit parameters correspond to the fits to the power law $\Delta E/\gamma a^2 = k(d_{cc}/a)^{-m}$ (where d_{cc} is the distance between the centers of mass of the particles) shown in the insets of Figs. 7 and 9 in the main manuscript; some of the bond energies are plotted in Fig. 8 of the main manuscript. For the repulsive tip-to-side orientation, the largest repulsive energy for direct contact of the particles is provided instead of a bond energy.

particle shape	**aspect ratio**	**orientation**	θ_c	**k**	**m**	**bond energy** $\Delta E/\gamma a^2$
Ellipsoidal	2	S-S	50°	-0.0415	2.81	-0.00578
			80°	-0.0080	2.69	-0.00122
		T-T	50°	-3.2039	5.21	-0.00241
			80°	-3.4804	6.03	-0.00087
		T-S	50°	0.2342	3.83	0.00349
			80°	0.0421	3.56	0.00084
	3	S-S	50°	-0.0863	2.07	-0.01975
			80°	-0.0117	1.92	-0.00298
		T-T	50°	-310.682	6.03	-0.00667
			80°	-489.442	7.02	-0.00181
		T-S	50°	1.89	3.73	0.01081
			80°	0.2694	3.55	0.00196
Cuboidal	3	S-S	40°	-0.0278	1.90	-0.00744
			60°	-0.0355	1.84	-0.00989
		T-T	40°	-107.6	5.70	-0.00395
			60°	-478.773	6.28	-0.00626
		T-S	40°	1.2484	3.80	0.00643
			60°	1.5979	3.72	0.00925

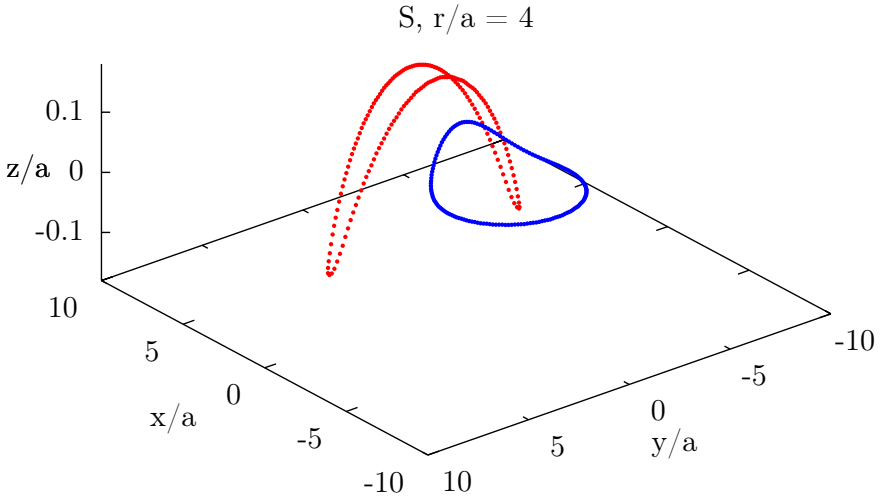

(a)

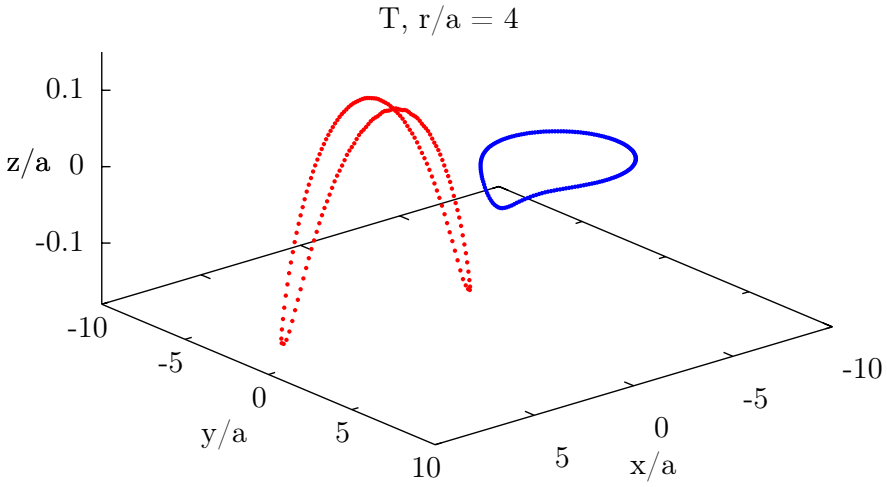

(b)

Figure S4: Contact line deformations for a spherical particle of radius $r = 4a$ and an ellipsoidal particle of aspect ratio $b/a = 5$ at a fluid interface with contact angle $\theta_c = 48.47°$ for both particles. The spherical particle approaches the ellipsoidal particle (a) at the side and (b) at the tip.

References

(1) Loudet, J.; Pouligny, B. How do mosquito eggs self-assemble on the water surface? *Eur. Phys. J. E* **2011**, *34(8)*, 1–17.

(2) Lehle, H.; Noruzifar, E.; Oettel, M. Ellipsoidal particles at fluid interfaces. *Eur. Phys. J. E* **2008**, *26*, 151–160.